Enhanced Electrochemical Performance of Supercapacitors via Two-Dimensional Indium Sulfide Heterostructure on Carbon Nanotubes

Niraj Kumar [1,†], Dhananjay Mishra [1,†], Ajit Kumar [1], Bidyashakti Dash [1], Rajneesh Kumar Mishra [2,*], Junyoung Song [1,*] and Sung Hun Jin [1,*]

1 Department of Electronics Engineering, Incheon National University, Incheon 22012, Republic of Korea
2 Department of Physics, Yeungnam University, Gyeongsan 38541, Republic of Korea
* Correspondence: rajneeshmishra08@gmail.com (R.K.M.); jun.song@inu.ac.kr (J.S.); shjin@inu.ac.kr (S.H.J.); Tel.: +82-32-835-8865 (S.H.J.)
† These authors contributed equally to this work.

Keywords: 2D materials; In_2S_3 nanostructure; SILAR deposition; supercapacitor

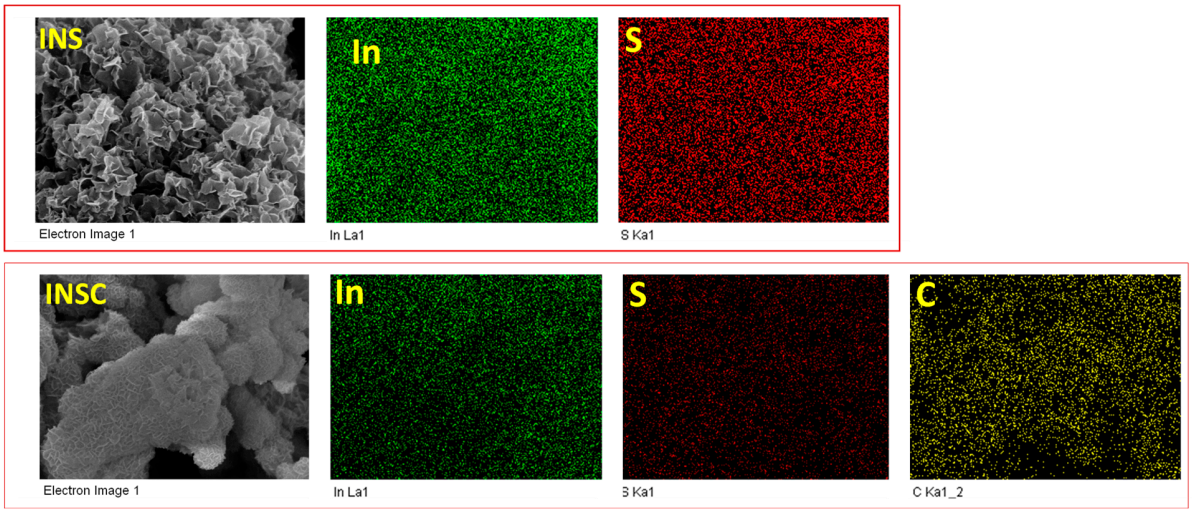

Figure S1. EDAX color mapping images of INS and INSC samples.

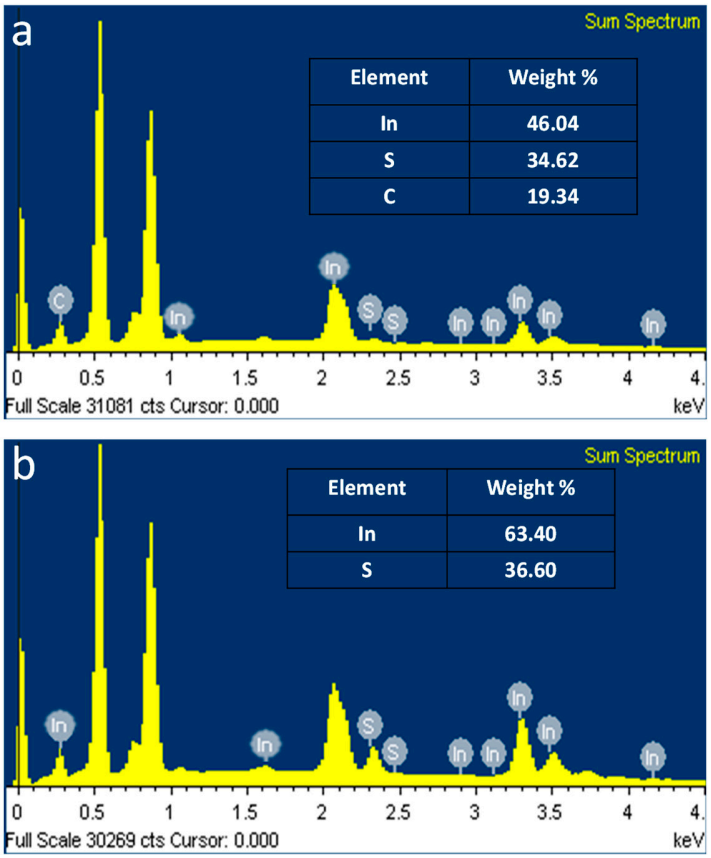

Figure S2. EDAX spectra of (a) INSC and (b) INS samples.

The reason for the change in In/S ratios between INS and INSC could be due to various reasons, such as: SWCNTs are carbon-rich materials, and they can dominate the EDS signal. SWCNTs contain a high concentration of carbon atoms, which makes it difficult to distinguish other elements within the sample.

Also, SWCNTs can alter the surface chemistry of the material. The addition of SWCNTs to a material can change its surface chemistry, leading to different chemical species being present on the surface. These changes can alter the X-ray signals detected during EDS elemental mapping, resulting in variations in the elemental distribution. Therefore, the presence of SWCNTs in a material can affect the accuracy of EDS elemental mapping. However, we get an idea of the presence of In, S, and C in the INSC sample.

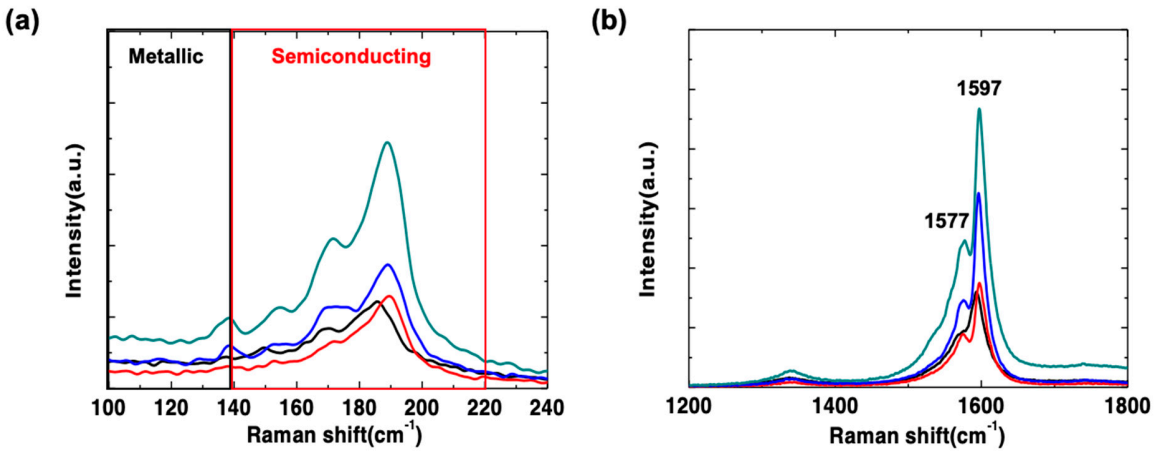

Figure S3. a) Raman RBM and b) spectra at the excitation wavelength of 532 nm for four randomly chosen points on the sample coated with SWNTs.

Raman spectra, excited via laser with a wavelength of 532 nm, clearly show semiconducting carbon nanotubes are rich on the film of SWCNTs in this study. Thus, FE-SEM images as well as the Raman study clearly substantiate that all samples in this work surely contain SWCNTs.

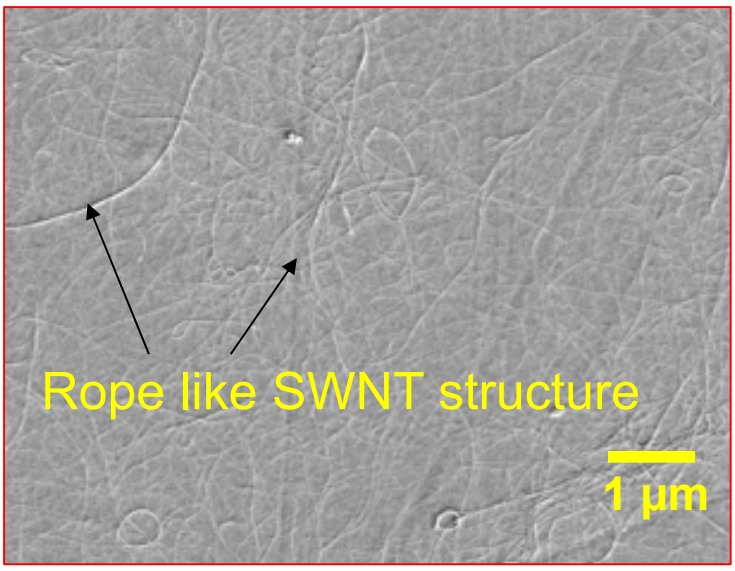

Figure S4. FE-SEM image of a SWCNT sample showing rope like SWNT.

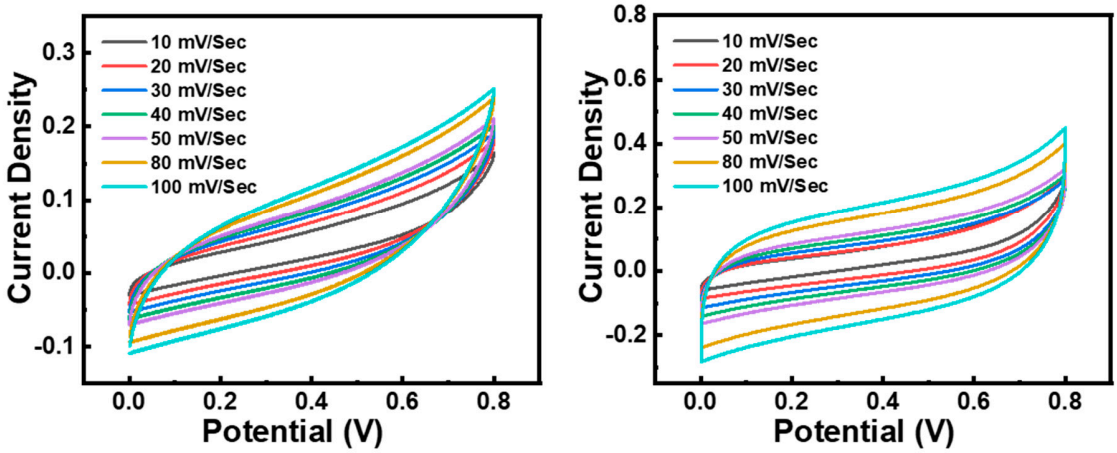

Figure S5. CV curves at different scan rates (10 mVs^{-1} to 100 mVs^{-1}) of (a) INSC and (b) INSC-based SCs.

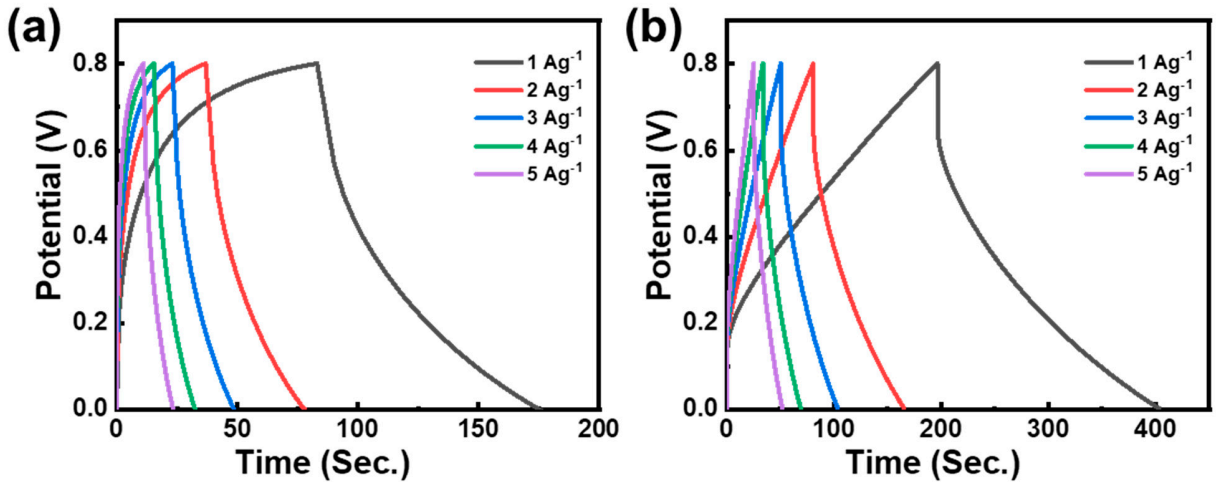

Figure S6. 2T GCD curves of sample INSC at (a) lower scan rates (1 Ag^{-1} to 5 Ag^{-1}) and (b) a higher scan rate range (1 Ag^{-1} to 100 Ag^{-1}).

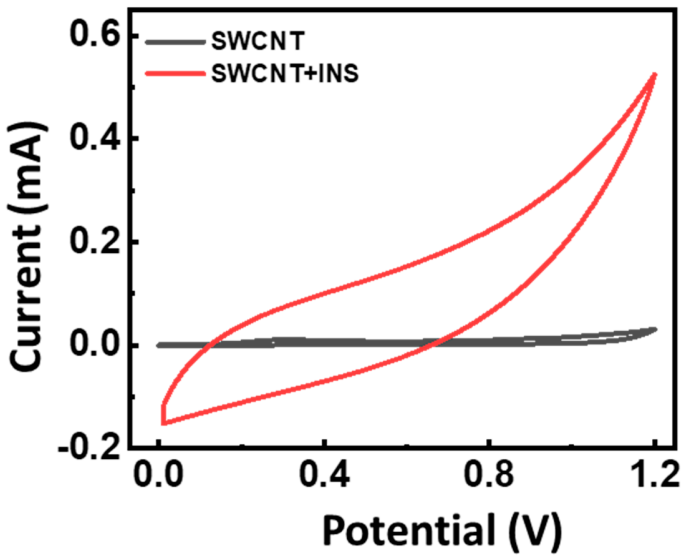

Figure S7. Comparative CV curves of bare SWCNT and INSC in a potential window of 1.2V.

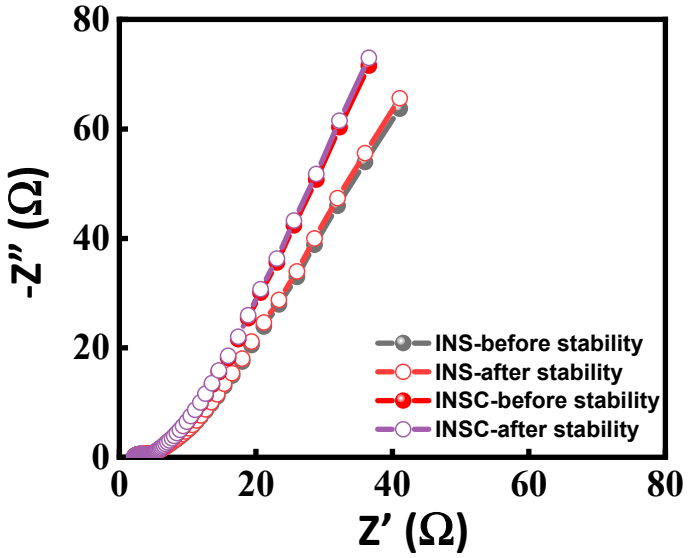

Figure S8. EIS test before and after the stability test.

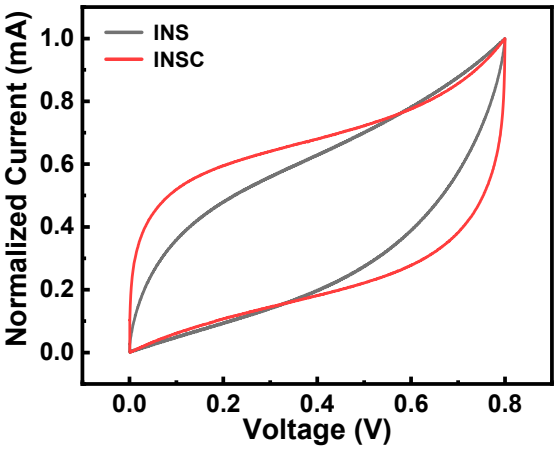

Figure S9. Normalized CV curves for INS and INSC samples at a scan rate of 100 $mV.s^{-1}$.

Table S1. Comparison between previously published indium electrode materials and the current work on electrochemical properties.

Electrode Material	Morphology	Synthesis Method	Specific Capacitance	Cyclic Stability (No. of Cycles)	Reference
In_2O_3	Nanowires	Chemical Vapor Deposition	16.6 mF cm^{-2}	66.8 (1000)	[1]
In_2O_3	Thin Layer	Atomic Layer Deposition	1.36 mF/cm^2	47.8 (2,000)	[2]
Indium Oxide	Hollow Spheres	Hydrothermal	30.84 F/g	86 (3,500)	[3]
In_2O_3/rGO	Aggregated Nanoparticles	Chemical Reaction	105 F/g	93.7 (5,000)	[4]
In_2O_3	Nanodiscs	Hydrothermal	89.7 F/g	97 (10,000)	[5]
InP_3	Layered	Liquid Phase Exfoliation	27.2 F cm^3	88.7 (10,000)	[6]
In_2S_3	2D Layered	Solvothermal	284 Fg^{-1}	90.81 (10,000)	[7]
M-In_2O_3	Nanoflake	Cation substitution route	128 Fg^{-1}	96 (5,000)	[8]
GNPs	-	Push coating	176F.g^{-1}	-	[9]
INSC	2D Layered Interconnected	SILAR	258 Fg^{-1}	96.83 (3,000)	This Work

Table S2 contains all of the impedance parameters estimated from the EIS graph.

Table S2. Impedance parameters estimated from the Nyquist plot of samples INS and INSC.

Sample	**R_s (Ω)** **Series Resistance**	**R_{ct} (Ω)** **Charge-Transfer Resistance**	**W (Ω)** **Warburg Resistance**	**C_p (F)** **Capacitance**
INS	0.46	1.84	0.87	1.16
INSC	0.36	1.61	0.74	1.34

References

[1] F.N. Tuzluca, Y.O. Yesilbag, M. Ertugrul, Synthesis of In 2 O 3 nanostructures with different morphologies as potential supercapacitor electrode materials, Applied Surface Science. 427 (2018) 956–964. doi:10.1016/j.apsusc.2017.08.127.

[2] B. Zhu, X. Wu, W.J. Liu, H.L. Lu, D.W. Zhang, Z. Fan, S.J. Ding, High-Performance On-Chip Supercapacitors Based on Mesoporous Silicon Coated with Ultrathin Atomic Layer-Deposited In 2 O 3 Films, ACS Applied Materials and Interfaces. 11 (2019) 747–752. doi:10.1021/acsami.8b17093.

[3] R. Kumar, A. Agrawal, T. Bhuvana, A. Sharma, Porous indium oxide hollow spheres (PIOHS) for asymmetric electrochemical supercapacitor with excellent cycling stability, Electrochimica Acta. 270 (2018) 87–95asymmetric electrochemical supercapac. doi:10.1016/j.electacta.2018.03.076.

[4] X. Xu, T. Wu, F. Xia, Y. Li, C. Zhang, L. Zhang, M. Chen, X. Li, L. Zhang, Y. Liu, J. Gao, Redox reaction between graphene oxide and in powder to prepare In 2O3/reduced graphene oxide hybrids for supercapacitors, Journal of Power Sources. 266 (2014) 282–290. doi:10.1016/j.jpowsour.2014.05.051.

[5] R.K. Mishra, J.H. Ryu, H.I. Kwon, S.H. Jin, Novel two-dimensional In2O3 nanodiscs for high-rate performance of solid-state symmetric supercapacitors, Materials Letters. 218 (2018) 131–134. doi:10.1016/j.matlet.2018.01.173.

[6] Y. Chang, B. Wang, Y. Huo, K. Zhai, L. Liu, P. Li, A. Nie, C. Mu, J. Xiang, Z. Zhao, F. Wen, Z. Liu, Y. Tian, Layered porous materials indium triphosphide InP3 for high-

performance flexible all-solid-state supercapacitors, Journal of Power Sources. 438 (2019) 227010. doi:10.1016/j.jpowsour.2019.227010.

[7] N. Kumar, D. Mishra, S. Yeob Kim, T. Na, S. Hun Jin, Two dimensional, sponge-like In2S3 nanoflakes aligned on nickel foam via one-pot solvothermal growth and their application toward high performance supercapacitors, Materials Letters. 279 (2020) 128467. doi:10.1016/j.matlet.2020.128467.

[8] I. Hussain, T. Hussain, C. Lamiel, K. Zhang, Turning indium oxide into high-performing electrode materials via cation substitution strategy: Preserving single crystalline cubic structure of 2D nanoflakes towards energy storage devices, Journal of Power Sources. 480 (2020) 228873. doi:10.1016/j.jpowsour.2020.228873.

[9] L.F. Aval, M. Ghoranneviss, G.B. Pour, Graphite nanoparticles paper supercapacitor based on gel electrolyte, Materials for Renewable and Sustainable Energy. 7 (2018) 1–11. doi:10.1007/s40243-018-0136-6.